Short running title: Land-use shapes P cycle genes in Amazon

Title: Land-use intensification reshapes microbial phosphorus cycling, organic matter composition and phosphorus fractions in Amazonian soils

Guilherme Lucio Martins [1,2,3*]; Gabriel Gustavo Tavares Nunes Monteiro [1,3]; Markus Lange [3]; Anderson Santos de Freitas [1]; Luana do Nascimento Silva Barbosa [1,2]; Johannes van Leeuwen [4]; Jorge Emídio de Carvalho Soares [4]; Rogério Eiji Hanada [4]; Gerd Gleixner [3]; Siu Mui Tsai [1]

[1] Center for Nuclear Energy in Agriculture (CENA), University of São Paulo (USP), Piracicaba, São Paulo, Brazil

[2] "Luiz de Queiroz" College of Agriculture (ESALQ), University of São Paulo (USP), Piracicaba, São Paulo, Brazil

[3] Department of Biogeochemical Processes, Max Planck Institute for Biogeochemistry, Jena, Germany

[4] Graduate Program in Agriculture in the Humid Tropics, National Institute for Amazonian Research (INPA), Manaus, Amazonas, Brazil

* **Corresponding author**: Guilherme Lucio Martins (guilhermelucio@usp.br / glucio@bgc-jena.mpg.de), Cell and Molecular Biology Laboratory, Center for Nuclear Energy in Agriculture, University of São Paulo, Av. Centenário 303, 13146-000, Piracicaba, São Paulo, Brazil

Abstract

Soil phosphorus (P) is a limiting factor for vegetation growth in the Amazon rainforest, where plants depend on microorganisms for organic matter cycling and nutrient uptake. While forest-to-agriculture conversion fundamentally reshapes plant-microbe-soil interactions and P cycling, these dynamics are further modulated by the intensity of land management. This study examined the 30-year effects of converting a primary forest into two contrasting systems: a low-intensity agroforest and a high-intensity citrus monoculture. We investigated how microbial and low molecular weight organic compounds (LMWC) composition interacted with soil physicochemical attributes, acid phosphatase activity, and P fractions (labile, moderately labile, non-labile, and residual). Agroforest soils retained physicochemical and enzymatic attributes similar to the primary forest, while soils of the citrus plantation showed increased P in all fractions due to mineral fertilization and reduced soil organic matter content, mainly in deeper layers. Microbial and LMWC composition patterns reflected land-use, with agroforest representing an intermediate state between primary forest and citrus monoculture. Pseudomonadota and nutrient-rich LMWC were more abundant in the agroforest, whereas Ascomycota and nutrient-poor LMWC predominated the citrus plantation. Genes related to “P acquisition” were more abundant in forest and agroforest soils, while genes related to “P-compound synthesis” were more abundant in the citrus plantation. Labile P was negatively correlated with genes related to microbial metabolism,

suggesting that reduced P availability may induce a boost in microbial activity for internal P-cycling. These findings demonstrate that forest-to-agriculture conversion strongly affects microbial functions, with responses aligning with land-use intensity and LMWC resource availability. Nonetheless, microbes adapt by shifting strategies: prioritizing mineralization and solubilization or favoring biosynthesis depending on P availability.

Keywords: Tropical forest; Biogeochemistry; Metagenomics; Hedley fractionation; Orbitrap; High-resolution mass spectrometry.

1. Introduction

The Amazon rainforest has experienced extensive deforestation in recent decades, disrupting essential plant-soil-microbes interactions that sustain ecosystem functions [1, 2]. The primary driver of land-use change in the region is the conversion of primary forests into agricultural and pastoral systems, often through slash-and-burn practices [3]. This transition alters the soil chemical, physical, and biological attributes and not only increases but also intensify soil degradation [4, 5]. The combined loss of vegetation and soil organic matter, along with the nutrient volatilization, immobilization, and leaching, severely diminishes long-term soil health in these low-fertility soils [6]. Further, Amazonian soils are acidic and highly weathered, conditions that are often accompanied by the presence of stable P minerals through strong geochemical binding to iron and aluminum hydroxides, causing low concentrations of bioavailable P [7]. As a result, P availability to plants is reduced, P becomes more recalcitrant, and microbial P cycling is altered [8, 9]. Given that most Amazonian soils are naturally nutrient-poor, P availability is considered a major constraint on plant productivity and ecosystem recovery following disturbance [10].

Therefore, sustainable agriculture is essential for preserving and maintaining ecosystem functions and biogeochemical cycles in events of land-use change. For instance, Amazonian agroforestry systems are often established on nutrient-poor soils, forcing plants to rely on strategies to overcome P limitations by recycling P through plant litter decomposition and microbial necromass [11]. In this sense, agroforestry integrates high plant diversity to optimize space and resource use, mimicking plant succession dynamics and above and belowground interactions as primary forests [12], which contrasts with monoculture. However, plant P uptake is limited to soluble inorganic P in form of orthophosphate, whereas most soil P exists in organic pools, such as litter, soil organic matter, and microbial biomass, as well as in inorganic forms adsorbed on soil particles with varying solubility [13]. However, despite their importance, the interactions between plants, microbes, and organic matter in P cycling remain poorly understood in different land use systems in the Amazon.

In this context, soil microbiota and LMWC compounds are important indicators of shifts in biogeochemical processes. LMWC consists of a complex mixture of plant- and microorganism-derived metabolites containing carbon, hydrogen, nitrogen, oxygen, phosphorus, and sulfur (CHNOPS) [14, 15]. It functions as both a source and a sink for organic compounds, and depending on its composition and stoichiometry between elements, provides energy and nutrients for microbial activity [16]. Although some microbe-derived compounds such as storage lipids, triacylglycerides and polyhydroxybutyrate only consist of CHO formulas, nutrient-rich LMWC typically presents low C:N ratios and high diversity of compounds, serving as a reservoir for newly microbially-synthesized products [17]. In contrast, nutrient-poor LMWC is mainly composed of plant-derived compounds containing only carbon, hydrogen and oxygen [18]. Consequently, LMWC may play an essential role in the P cycle, making it

fundamental to comprehend its interactions with soil microbial communities in systems undergoing land-use change in the Amazon. For example, plant-microbe interactions can contribute to nutrient retention and facilitate transformation of insoluble P fractions into labile forms available for plant uptake [9, 18]. As a result, LMWC stimulates microbial communities to perform nutrient cycling processes [19].

Microbial P-cycling involves hundreds of genes categorized into major "extracellular" and "intracellular" metabolic pathways [20]. The former is grouped into genes related to "P acquisition" which includes solubilization, mineralization, and transport of P. The later pathway includes genes related to synthesis of new "P-containing compounds", such as purine and pyrimidine metabolism and oxidative phosphorylation [21, 22]. While these pathways are regulated by environmental conditions, the mechanisms governing specifically bacterial and fungal P acquisition and turnover in tropical soils over long term of land-use change remain poorly understood. It is known that bacterial communities often respond stronger than fungal communities to P addition, and that P availability can influence microbial storage processes, including incorporation into membranes and DNA [23]. However, the functional pathways controlling these processes are not well elucidated.

Here, we investigate how land-use change, and management intensity affect microbial and LMWC composition, focusing on the abundance of P-cycling genes involved in both extracellular and intracellular processes, and their relationship with different soil P fractions. We hypothesize that: (i) microbial and LMWC composition are strongly related to land use; and (ii) microbial phosphorus cycling genes are shaped by LMWC composition and soil phosphorus fractions, but also affect them, creating a bi-directional hypothesis, with LMWC exerting a stronger effect than P fractions.

2. Material and Methods

2.1. Study site, Experimental Design and Management Intensity

The study was conducted in Manacapuru, Amazonas, Brazil (03º16'50" S; 60º30'17" W) (Fig. S1). The region has a Rainy Tropical (Amw) climate, according to the Köppen classification, with an annual average temperature of 28ºC, humidity of 75-85%, and annual rainfall of 1,750–2,500 mm [24]. The soils are classified as Ferralsol [25]. The study sites are part of the "Ramal do Laranjal" land reform settlement, established in 1989 by the municipality of Manacapuru.

The agroforest system was established during the rainy season of 1992/1993 and 1993/1994 as a sustainable agriculture initiative by the National Institute of Amazonian Research (INPA). The site is managed by a local farmer and consists of three vertical strata: (i) *Theobroma grandiflorum* and *Paullinia cupana* in the lower stratum; (ii) *Euterpe precatoria* and *Bactris gasipaes* in the middle stratum; and (iii) *Bertholletia excelsa* in the upper stratum. The citrus plantation was established in the rainy season of 1997 using seedlings grafted with orange (*Citrus* × *sinensis*) as the graft, and mandarin lime (*Citrus* × *limonia*) as rootstock. Initial fertilization included 300 g of lime and 100 g of P_2O_5 per pothole, with mostly annual applications of 50 g each of $CO(NH_2)_2$, P_2O_5, and K_2O per tree. A full description of the site's management history is presented in the supplementary material (Table S1). The primary forest, used as a reference, is a highly preserved forest adjacent to the land reform settlement and has remained undisturbed for over 50 years. The most dominant species were composed of *Protium hebetatum*, *Eschweilera coriacea*, *Licania oblongifolia*, and *Pouteria minima*. These species are considered as typical of *terra firme* dense forest in the Amazon [26].

Soil sampling occurred in May 2022 at the end of the wet season, due to the relative soil stability in moisture and peak microbial activity found in this period. A 60 × 60 m plot was established in each land-use system with five sampling points (four corners and center) to minimize edge effects. Five samples were collected per system at each soil depth (0–10 cm, 10–20 cm, and 20–30 cm) using a Dutch auger, totaling 45 soil samples. Undisturbed samples for bulk density and porosity were collected with metallic volumetric rings (8 × 5 cm) using an Uhland-type auger. For molecular analysis (DNA and LMWC), topsoil (0–10 cm) was collected in sterile centrifuge tubes, as this layer is considered a microbial activity hotspot compared to the subsoil layer [27]. Samples for enzymatic, chemical and physical analyses were stored at 4ºC, while molecular analyses samples were preserved at -20ºC.

2.2. Soil Chemical and Physical Analysis

Soil chemical attributes were analyzed following the procedures described in the literature [28]. Briefly, soil pH was measured in a $CaCl_2$ solution (0.01 mol L^{-1}). Soil organic carbon was quantified via oxidation using $K_2Cr_2O_7$ solution (0.07 mol L^{-1}). K^+, Ca^{2+}, and Mg^{2+} were extracted using ion exchange resins; K^+ was quantified using a colorimetric method, while Ca^{2+} and Mg^{2+} were measured by atomic absorption spectrophotometry (PerkinElmer 3100, USA). SO_4^{2-} was extracted with a $Ca_3(PO_4)_2$ solution (0.01 mol L^{-1}) and quantified by turbidimetry. Al^{3+} was extracted with a KCl solution (1.0 mol L^{-1}) and quantified by titration with NaOH solution (0.025 mol L^{-1}). Micronutrients, including Fe, Cu, Mn, and Zn, were extracted using diethylenetriaminepentaacetic acid (DTPA) and quantified via atomic absorption spectrophotometry. Cation exchange capacity (CEC) was estimated based on the sum of Ca^{2+}, Mg^{2+}, K^+, Al^{3+}, and H^+.

Soil physical attributes were analyzed according to the methods described in the literature [29]. Shortly, soil bulk density was determined from undisturbed samples collected using metallic volumetric rings (8 × 5 cm). Soil macroporosity was measured through capillary rise water saturation by weighing samples and transferring them to a tension table at −6 kPa until hydraulic equilibrium was achieved. Microporosity was determined by drying the same samples at 105°C for 48 hours and reweighing them.

Soil enzymatic activity was assessed by quantifying the amount of ρ-nitrophenol released during the incubation of substrates analogs in 1 g of soil at 37°C for 1 hour, using a 96-well microplate reader (LMR-96 Loccus, São Paulo, Brazil). Enzymatic activity was measured using substrates analogs: β-glucosidase activity was measured at 410 nm using ρ-nitrophenyl β-glucopyranoside (PNG) [30]. Acid phosphatase activity was measured at 420 nm using ρ-nitrophenyl disodium phosphate (PNP) [31]. Arylsulfatase activity was measured at 410 nm using ρ-nitrophenyl sulfate (PNS) [32].

2.3. Phosphorus Fractionation Techniques

Soil phosphorus (P) fractionation was conducted following [33], with modifications [34]. Sequential extraction was performed using 0.5 g of air-dried soil in the following order: labile P, which is readily available for plant uptake, was extracted using 10 mL of Mehlich-3 solution, followed by shaking for 1 hour on an end-over-end tube rotator at 30 rpm, centrifugation at 3600 × g for 15 min, and collection of the supernatant. Moderately labile inorganic P was extracted with 10 mL of NaOH solution (0.5 mol L^{-1}), followed by shaking for 1 hour, centrifugation for 15 minutes, and collection of the supernatant. Moderately labile organic P was obtained through autoclave digestion with 1 mL of H_2SO_4 (98%, analytical grade) and 0.75 g of $(NH_4)_2S_2O_8$ for 120 min. Non-labile P, primarily bound to calcium minerals, was extracted with 10 mL of HCl solution (1 mol L^{-1}), followed by shaking and centrifugation. Additionally, total P content

was determined using 0.1 g of soil. Samples were treated with 2 mL of H_2SO_4 (98%) and 2 mL of H_2O_2 (37%, analytical grade) and digested in heating blocks for 2 hours at 350°C. The P content in all fractions and total P were quantified using the colorimetric method [35]. Residual P, consisting of highly recalcitrant inorganic and organic forms that are largely unavailable to plants, was estimated as the difference between total P and the sum of the extracted fractions.

2.4. Low Molecular Weight Organic Compounds Extraction, and High-Resolution Mass Spectrometry

Low molecular weight organic compounds (LMWC) was obtained from topsoil (0–10 cm) following [36] with slight modifications. This method was adopted to extract compounds held in the solution and exchange phase, as well as to avoid the biodegradation of low weight molecular compounds by microbes [36]. Briefly, 4.0 g of field-moist soil was mixed with 20 mL of KCl (2.0 mol L^{-1}) (1:5 w/v), shaken at 20ºC for 1 hour at 200 rpm, centrifuged at 8000 × g for 10 min. The supernatant was collected and filtered through a 0.45 µm glass fiber syringe filter (Whatman, Maidstone, UK), and extracts were acidified to pH 2.0 with HCl (37%, Sigma-Aldrich, USA). The concentration of dissolved organic carbon (DOC) was quantified using a TOC analyzer (Shimadzu, Japan). The LMWC extracts were isolated using Agilent Bond Elute PPL Solid Phase Extraction (SPE) cartridges (100 mg) [37]. Injection volumes were normalized to sample DOC concentrations to achieve a constant load of 200 µg C per cartridge. Compounds were eluted with ultrapure methanol, and SPE extraction efficiency was assessed on a Vario TOC cube analyzer (Elementar, Germany) [18]. Blank samples containing ultrapure water were included and treated in the same way as the samples to identify and exclude background signals unrelated to LMWC.High-resolution mass spectrometry (HR-MS) was performed using an Orbitrap Elite (Thermo Scientific),

following [15, 38, 39]. The instrument was operated with direct injection of 100 µL of PPL-extract into the autosampler at a flow rate of 20 µL min^{-1}, using a solvent mixture of ultrapure water and methanol (1:1). Electrospray ionization (ESI) was performed in negative mode with a voltage of 2.65 kV, without a separation column. Spectra were collected over a mass-to-charge (m/z) range of 100–1000.

An average of 100 scans per sample was combined into a single average mass spectrum and converted into spectral peaks using Thermo Xcalibur software (v. 3.0.63). ThermoRawFileParser software (v.1.7.4) [40] converted raw files to *mzML* format, retaining only m/z values with a signal-to-noise ratio >6 for further analysis.

2.5. Low Molecular Weight Organic Compounds Analysis

Formula assignment was conducted using internal recalibration of spectral peaks with the *MFAssignR* package [41]. Ions with m/z values between 150–500 were considered for recalibration as approximately 80% of the accumulated intensity of the respective spectrum was reached within this range [42]. The sum formulae assignment was performed under the following conditions: ^{12}C: 1–70, ^{1}H: 2–160, ^{16}O: 0–70, ^{14}N: 0–7, ^{32}S: 0–3, ^{31}P: 0–3, and a tolerance of ± 0.5 ppm. This process resulted in the assignment of 9710 formulae across 15 samples. From these formulae, we determined key molecular metrics, including the hydrogen-to-carbon ratio (H/C), oxygen-to-carbon ratio (O/C), carbon-to-nitrogen ratio (C/N), modified aromaticity index (AImod), aromatics metabolites [43], nominal oxidation state of carbon (NOSC) and the difference between double bond equivalency and oxygen atom count (DBE-O) [44].

2.6. DNA Extraction and Sequencing Protocols

Total DNA was extracted from topsoil (0–10 cm) using 0.25 g of soil. Extraction was performed with PowerSoil Pro Kit (Qiagen, Hilden, Germany), following

manufacturer's protocol. DNA quantity and quality were measured using a Nanodrop 2000c spectrophotometer (Thermo Fisher, USA), and DNA integrity was confirmed by 1% agarose gel electrophoresis at 90 V for 30 min.

For amplicon sequencing, 16S rRNA gene and ITS region were targeted to analyze prokaryotic and fungal communities, respectively. The V3–V4 hypervariable region of the 16S rRNA was amplified using the 515F/806R primers [45], while the ITS region was amplified using the ITS1f/ITS2 primers [46]. Library was constructed using the Illumina NextSeq 1000/2000 P1 Reagent kit (Illumina, San Diego, USA). PCR reactions followed the Nextera XT Kit protocol (Illumina, San Diego, USA), and DNA amplification was confirmed by gel electrophoresis. Purified amplicons were equimolarly pooled, and the library's final concentration was determined using a SYBR green quantitative PCR assay with primers specific to the Illumina adapters Kapa (KAPA Biosystems, Boston, USA). Finally, sequencing was carried out on the Illumina NextSeq platform (Illumina, San Diego, USA) with a length of 2 × 250 bp paired-ended reads.

Shotgun metagenomics was performed on the Illumina HiSeq 2500 platform (Illumina, San Diego, USA) with the HiSeq Reagent Kit v.4, following the manufacturer's recommendations. DNA libraries were constructed using 2 μg of DNA per sample, fragmented to sizes lower than 500 bp. DNA fragments were amplified by PCR using P5 and P7 primers for multiplexing and subsequently purified and quantified using a Qubit 2.0 fluorometer (Invitrogen, Carlsbad, USA). Finally, libraries were multiplexed and sequenced with paired-end reads of 2 × 100 bp.

2.7. Microbial Community and Functioning Analysis

Processing of amplicon sequencing data, including quality control, reconstruction of 16S rRNA and ITS genes, and taxonomic annotations, was conducted using the *nf-*

core/ampliseq pipeline (v.2.11.0) [47, 48]. The pipeline was run with default settings, employing Cutadapt (v.1.16) to remove primers, QIIME2 for sequence import, and the DADA2 algorithm [49] for sample processing. Sequences with a quality score below 30 and PCR chimeras were discarded, and a minimum read frequency of three was applied to exclude singletons and doubletons. Taxonomic annotation was performed using the SILVA database (v.138) for prokaryotes and the UNITE database (v.9.0.) [50] for fungi. Taxa classified as Archaea and Eukaryote were removed from the prokaryotic dataset. The sequences are available at the NCBI Sequence Read Archive under the identification PRJNA1244318.

Metagenomics functional profile was assessed with the DiTing pipeline (v.0.9) [51] to analyze the relative abundance and occurrence of metabolic and biogeochemical pathways related to microbial P cycling. Briefly, reads were assembled using MEGAHIT (v.1.1.3) [52], and open reading frames (ORFs) were predicted from contigs using Prodigal (v.2.6.3) [53]. ORFs annotations were conducted using the KEGG ortholog database with HMMER3 (v.3.4). The relative abundance of KOs was obtained by mapping the ORF against the metagenomic reads, with results expressed as sequences per million (SPM).

2.8. Statistical Analysis and Data Interpretation

All statistical analyses and visualizations were conducted in R (v.4.4.1). Soil attributes were tested for normality with the Shapiro-Wilk test and homoscedasticity of residuals with the Levene's test to assess their suitability for parametric analysis. When assumptions were met, differences between land-use systems were tested using one-way ANOVA, followed by Tukey's HSD test ($p < 0.05$) for post-hoc comparisons. Otherwise, the Kruskal-Wallis test was applied, followed by Dunn's post-hoc test ($p < 0.05$).

Data were standardized using Z-score normalization, and Principal Component Analysis (PCA) was subsequently performed on the resulting correlation matrix using the *factoextra* package [54] to evaluate differences in soil chemical attributes across land-use systems. Principal Coordinate Analysis (PCoA) based on Bray-Curtis dissimilarity was performed to examine microbial and LMWC composition, using the *vegan* package [55]. Differences in microbial and LMWC compositions were assessed with PERMANOVA using the *pairwiseAdonis* function ($p < 0.001$) and interpreted by the coefficients of determination (R^2). The relative abundance of bacteria, fungi, and LMWC were transformed in centered log-ratio (*clr*) and means were compared by the Kruskal-Wallis test, using the *ALDEx2* package [56]. Heatmaps based on Spearman correlation ($p < 0.0001$) were generated to evaluate the relationships between P-cycling genes and P fractions, and between LMWC and P fractions, using the *corrplot* package.

Partial Least Squares Path Modeling (PLS-PM) [57] was performed to explore the effects of microbial and LMWC composition on P-cycling pathways and their relationship with P fractions. A complete description of the paths and hypothesis behind the model is described in the supplementary files (Table S2). The *plspm* package [58] was used to estimate the strength of path coefficients (i.e., direct effects) and coefficients of determination (R^2) for linear relationships among variables, using 1000 bootstraps for validation. Model assumptions were checked via *unidimensionality* (Cronbach's alpha > 0.7) using the *outerplot* function, the commonality of latent variables (commonality > 0.49) through cross-loading scores. The final model structure was visualized using the *innerplot* function.

3. Results

3.1. Land-use change impacted soil attributes and phosphorus fractions

Principal component analysis (PCA) revealed distinct soil chemical differences across the land-use systems, with the first two principal components explaining 66.6% of total variation (Fig. 1A). The first axis separated the citrus plantation from the primary forest and the agroforest, mainly due to higher concentrations of magnesium (Mg) and calcium (Ca) in the first soil depth (Fig. 1B). Citrus soils showed higher pH, as well as elevated concentration of manganese (Mn) and zinc (Zn), while the primary forest and agroforest soils showed higher concentrations of aluminum (Al^{3+}), boron (B), and cation exchange capacity (CEC) (Fig. 1B; Table S3). Variation along the second axis corresponded to differences between soil depths, with upper-layer samples characterized by higher concentrations of soil organic matter (OM), iron (Fe), and potassium (K). (Fig. 1B; Table S3).

Soil biological attributes also varied across land-use systems and soil depths (Fig. 1C). Acid phosphatase activity was highest in forest soils, followed by the agroforest and citrus plantation at all depths. Beta-glucosidase activity showed no significant differences among sites in the top two soil layers (0–10 cm, 10–20 cm) but was significantly higher in primary forest and agroforest soils compared to citrus plantation at 20–30 cm. In contrast, arylsulfatase activity was highest in citrus plantation at 0–10 cm but lower than forest and agroforest at deeper layers. Soil physical attributes differed mainly in deeper layers (Fig. S2). Total porosity was significantly higher in agroforest soils than in forest and citrus plantation soils in the second and third depths, while soil bulk density was significantly higher in citrus at 10–20 cm and 20–30 cm. No significant differences were observed in the topsoil.

Phosphorus fractions varied significantly after long-term forest conversion (Fig. 2). Citrus plantation soils exhibited higher total P content and higher concentration of P in all extractable fractions compared to primary forest and agroforest in all three layers.

In the topsoil layer (0–10 cm), the agroforest had a similar total P content to citrus plantation but showed the lowest concentration in the deepest layer (20–30 cm). The majority of P across all sites was found in the organic fraction at all soil depths. Citrus plantation soils also contained higher levels of inorganic moderate labile and labile phosphorus at all depths. In contrast, primary forest and agroforestry soils had higher residual phosphorus content compared to citrus plantation.

3.2. Microbial and LMWC composition across different land-use systems

A total of 3966 bacterial ASVs were identified, with an average of 82098 reads per sample after quality control analysis. Pseudomonadota was significantly more abundant in primary forest compared to other sites, Acidobacteriota was more abundant in agroforest, although differences were not significant, while Chloroflexota was significantly higher in citrus plantation (Fig. S3). For fungi, 7724 ASVs were identified, averaging 111620 reads per sample. Ascomycota and Basidiomycota comprised over 70% of the fungal community, though many taxa remained unclassified at phylum level. Ascomycota was the most abundant phylum for all sites although differences were not significant, while Basidiomycota was significantly more abundant in primary forest and agroforest, and Glomeromycota was higher in citrus plantation (Fig. S3).

Microbial composition differed significantly across land-use systems after long term forest-to-agriculture conversion (Fig. 3). Bacterial composition showed the most pronounced differences between primary forest and citrus plantation (PERMANOVA R^2 = 0.45), followed by primary forest and agroforest (R^2 = 0.41), and agroforest and citrus plantation (R^2 = 0.33) (Fig. 3A). Bray-Curtis distance analysis revealed that bacterial composition was more homogeneous in agroforest compared to citrus plantation due to lower dissimilarity indices (Fig. S4). Similarly, fungal communities exhibited the most pronounced differences between primary forest and citrus plantation (R^2 = 0.32), while

the differences between primary forest and agroforest, as well as between agroforest and citrus plantation, were identical ($R^2 = 0.24$) (Fig. 3B). However, the Bray-Curtis distance revealed that the fungal composition was more heterogeneous in agroforest soils than in citrus plantation (Fig S4).

For LMWC, 9710 molecular formulas were identified, comprised primarily by CHO (carbon, hydrogen, and oxygen), and CHNO (carbon, hydrogen, oxygen, and nitrogen) formulas, which together represented 96% of the total assigned formulas in the LMWC composition (Fig. S3). Although there were no significant site differences, CHO formulas increased by an average of 12.4%, and CHNO formulas decreased by an average of 13.3% in citrus soils compared to primary forest soils. LMWC composition showed different patterns from microbial community composition (Fig. 3C). The strongest differences in LMWC composition occurred between agroforest and citrus plantation ($R^2 = 0.34$), followed by comparisons between the primary forest and citrus plantation ($R^2 = 0.32$), and between the primary forest and agroforest ($R^2 = 0.19$). Among the LMWC parameters, the hydrogen-to-carbon (H/C) ratio had a higher relationship with primary forest soils, while phosphorus-to-carbon (P/C) ratio was more related to citrus plantation soils. The mass-to-charge ratio (m/z) and the nominal oxidation state of carbon (NOSC) were by tendency separated both agroforest and primary forest soils from the citrus plantation.

3.3. Phosphorus cycling genes and pathways across different land-use systems

A total of 92 genes involved in P-cycle were identified across land-use systems (Fig. 4A). The most abundant genes were *pyrG* (encoding the orotidine-5′-decarboxylase), *pstS* (phosphate-binding protein), *guaA* (glutamine amidotransferase), and *prsA* (post-translocation molecular chaperone). Land-use influenced the majority of P-cycling genes, with distinct patterns observed: genes increased in primary forest were

decreased in citrus plantation, while genes decreased in primary forest were increased in citrus. Agroforest exhibited intermediate levels of gene abundance compared to the other two systems.

The highest sequence abundance was associated with purine metabolism, followed by pyrimidine metabolism, the pentose phosphate pathway, and transporters (Fig. 4B). Genes related to the "P-compounds synthesis" pathway, such as the purine and pyrimidine metabolism, and the oxidative phosphorylation, were significantly increased in the citrus plantation compared to the primary forest and agroforest. In contrast, genes related to the "P acquisition" pathway, which included transporters, phosphonate, and phosphinate metabolism, were significantly higher in the primary forest than in both the agroforest and citrus plantation.

3.4. Environmental drivers of phosphorus cycling genes

P-cycling pathways and LMWC composition had significant relationships with different soil P fractions (Fig. S5). The organic and residual P fractions showed contrasting correlation patterns. The organic P fraction was positively correlated with several P-cycling pathways, such as pyrimidine metabolism, purine metabolism, and oxidative phosphorylation, as well as with LMWC composition such as CHP and CHOSP compounds. In contrast, the residual P fraction showed positive correlations with pathways including the pentose phosphate pathway, transporters, and phosphonate and phosphinate metabolism. Further correlations showed that P-cycling pathways were also affected by the LMWC composition (Fig. S6). The strongest positive correlations were observed between pyrimidine metabolism and CHP compounds ($\rho = 0.71$), followed by two-component system and CHNP ($\rho = 0.65$), and purine metabolism and CHP ($\rho = 0.60$). Conversely, the strongest negative correlations were observed between phosphonate and

phosphinate metabolism with CHP (ρ = -0.75), followed by organic phosphoester hydrolysis and CHNOS (ρ = -0.63).

PLS-PM analysis revealed that both microbial and LMWC composition influenced the abundance of genes associated with the "P acquisition" and "P-compound synthesis" pathways, which in turn affected soil P fractions (Fig. 5A and Table S4). Path analysis showed that microbial composition had a stronger overall effect on P-cycling genes than LMWC composition. Specifically, the first PCoA axis for bacteria and fungi, representing microbial composition, was positively correlated with the "P-compounds synthesis" pathway (0.58) and negatively correlated with the "P acquisition" pathway (-0.76). In contrast, LMWC composition showed weaker correlations with these pathways (0.57 and -0.17, respectively). Microbial composition was also positively correlated with both labile P fraction (0.82) and the moderate labile P fraction (0.83), while LMWC composition did not significantly influence either P fraction. The two microbial P-cycling pathways showed contrasting effects on P availability. The "P acquisition" pathway was positively correlated with moderately labile P (0.60), whereas the "P-compound synthesis" pathway was negatively correlated with labile P (-0.78).

PLS-PM analysis also revealed the reverse relations, showing that labile and moderate labile P fractions significantly influenced microbial and LMWC composition (Fig. 5B and Table S5). Specifically, the moderate labile P fraction had a stronger and significant effect on P-cycling pathways, exhibiting a positive correlation with the "P acquisition" pathway (0.91) and a negative correlation with the "P-compound synthesis" pathway (-0.74). In contrast, the labile P fraction did not significantly affect either pathway. Additionally, the "P acquisition" pathway showed a negative correlation with microbial composition (-0.43), while LMWC composition was not significantly influenced by any P-cycling pathway.

4. Discussion

This study investigated the influence of microbial and LMWC composition on P-cycling genes and P fractions across different Amazonian land-use systems, unlike most of the current works in the field, which are attached to non-forests environments [59, 60]. As hypothesized, land-use change significantly altered soil physicochemical attributes, microbial composition and function, and the LMWC profile, primarily driven by changes in nutrient availability. However, the conversion of forest to agroforest mitigated the impacts on both biotic and abiotic soil attributes compared to the more intensive citrus plantation. P-cycling genes showed distinct correlations with soil P fractions: the "P acquisition" pathway positively correlated with moderate labile P, while the P-compounds synthesis" pathway negatively correlated with labile P. These results highlight the adaptive role of soil microbes to regulate P cycling processes in response to changes in LMWC composition and resource availability [14, 18]. Overall, our findings suggest that land management practices can influence microbial function and improve P-use efficiency, even in nutrient-poor soils like those in the Amazon.

4.1. Microbial and organic matter composition patterns after long-term land-use change

Land-use change has well-documented impacts on Amazonian soil attributes and microbial composition [9, 61, 62]. However, this study provides a novel perspective on ecosystem functioning by demonstrating that LMWC composition differs from microbial composition patterns and provides important insights into biogeochemical processes. For instance, the conversion of primary forest into an agroforest maintained a homogeneous bacterial community with a lower dissimilarity index, while converting into a citrus plantation resulted in the homogenization of fungal communities (Fig. S4). In contrast, LMWC composition was more dependent on plant species composition, as the agroforest

was more homogeneous compared to the primary forest, with citrus monoculture positioned in an average dissimilarity between the other two groups. This suggests that changes in vegetation could mainly trigger responses in rhizosphere bacteria and saprophytic fungi, thereby further shaping the LMWC composition [18, 63]. These compositional shifts are likely influenced by reduced soil organic matter content [64] but also by high management intensity practices, such as fertilization and liming in citrus plantations [65, 66]. Moreover, microbial divergence aligned with environmental drivers, as bacterial communities tend to respond to nutrient availability, and fungal communities respond to aboveground vegetation [12]. These results emphasize the potential to influence the soil microbiome through vegetation manipulation, as promoting plant diversification enhances a broader fungal community, and improving nutrient availability supports bacterial community development [67].

In this context, the observed microbial patterns reinforce our first hypothesis that microbial and organic matter composition are tightly linked to land-use change. For example, we observed an increased abundance of Chloroflexota in the citrus plantation, which is often correlated with reduced organic carbon and nitrogen levels [68], while the higher abundance of Acidobacteriota in the agroforest could correspond to lower pH and organic matter-rich conditions [69, 70]. This group is especially important in highly weathered soils due to their tolerance to aluminum toxicity [71], a common condition observed in tropical soils. Such shifts in microbial distribution may indicate declining soil health, as these changes involve transitions from oligotrophic to copiotrophic taxa; e.g., from Ascomycota to Basidiomycota, or from Acidobacteriota and Chloroflexota to Pseudomonadota and Actinomycetota [72, 73]. Although microbial life strategies may not fit accurately into a binary classification of copiotrophic versus oligotrophic, especially at the phylum level [74], our data suggest that forest-to-agriculture conversion tends to

favor taxa adapted from high- to low-carbon soils. This shift is likely driven by intense soil management and by reductions in plant diversity and soil carbon, which can also decrease nutrient use efficiency [75]. Moreover, monoculture management, such as in the citrus plantation, can even amplify these effects.

The microbial composition patterns were also reflected in the LMWC composition, supporting the idea that organic compound diversity is shaped by specific plant and microbial inputs, as well as soil attributes [76, 77]. Our results suggest that LMWC transformation is primarily driven by the bacterial community [76, 78], as nutrient-rich compounds (e.g., CHNP formulas) were more prevalent in the agroforest, while nutrient-poor compounds (e.g., CHO formulas) dominated in citrus plantation (Fig. S3). These compositional changes were evident in H/C, N/C ratios, and NOSC in agroforest, which is often indicated as a result of greater microbial processing [79]. In addition, the decaying litter layer in the forest and agroforest likely influenced the resulting LMWC composition, in contrast with the citrus plantation, where the litter layer was absent (Fig. S8). Root exudates from citrus plants also contain substantial amounts of limonene and other terpenes, which may contribute to the higher CHO fractions observed in this system [80]. In summary, land-use change alters both microbial and LMWC composition, transitioning from nutrient-rich, microbially derived compounds to nutrient-poor, plant-derived compounds. However, transition to agroforestry appears to mitigate the adverse effects of land-use change, maintaining functionality close to that of primary forests.

4.2. Phosphorus cycling genes and phosphorus fractions after long-term land-use change

The long-term conversion of forest to agroforest and citrus plantation likely altered the soil P fractions by influencing the physical, chemical, and biological soil

attributes. Differences in land management intensity, such as altered plant diversity in agroforestry or the use of fertilizers in citrus plantations, may have further amplified these changes. Consequently, soil microbial communities and their associated P-cycling genes also diverged, reinforcing differences in soil P fractions.

However, despite annual fertilization in citrus plantations, total P concentrations remained critically low (< 200 mg kg^{-1}), which is concerning for agriculture in the Amazon, where over 60% of soils are classified as low-P Ferralsols [11, 81]. In the agroforest, total P in topsoil was similar to that of the citrus plantation but significantly lower in deeper layers, suggesting that plants could be more efficient at nutrient mining in the subsoil layers. However, soil P accumulated primarily in topsoil of agroforest, suggesting that these systems are highly dependent on soil health to ensure effective nutrient cycling, such as microbial activity, and total soil organic matter content [82, 83]. Moreover, agroforest soils showed higher litter biomass, litter P content (Fig. S7 and S8), and phosphatase activity than citrus plantation that had no litter layer, indicating enhanced P release through organic matter decomposition and stimulation of P-cycling microbes [84]. Furthermore, the reduced phosphatase activity in the citrus plantation may be linked to effects related to liming and P fertilization [85]. This was supported by a greater abundance of microbial genes involved in P mineralization and transport, reflecting efficient P recycling even under limited nutrient availability.

Our second hypothesis examined the cause-and-effect relationship of whether microbial communities influence P fractions by altering P-cycling genes, or whether P fractions drive microbial community composition. Overall, the effects of microbial and LMWC composition on P fractions were stronger than the effects of P fractions on microbial and LMWC composition. This reinforced the idea that microbial activity is directly related to resource availability in the organic matter pool, as microbial

composition was positively related to P availability. This suggested that under nutrient-poor LMWC conditions, low P availability stimulate internal P recycling mainly, primarily through microbial metabolism, and reduces microbial P release from cells [23]. In contrast, nutrient-rich LMWC and C:P ratios lower than 70:1 can stimulate the extracellular P-recycling [86], as pathways related to mineralization and transporter genes were enriched in the primary forest and agroforest sites. Consequently, the enrichment of P- and N-containing LMWC over CHO-LMWC in the agroforest is likely associated to fungal copiotrophs and with byproducts of microbial activity [18, 23]. Ultimately, these processes influence the concentrations of labile and moderately labile P fractions over long-term land use change.

Nevertheless, sequential P fractionation provides a more accurate assessment of plant-available P than identifying which soil properties affects the P fractions or the chemical forms of different P pools [87]. This may explain the stronger correlation between microbial communities and labile P, as well as the negative correlation between labile P and nutrient-poor LMWC. These results indicate that under P-limited conditions, microbial communities can access non-labile and residual P fractions and retains it in their intracellular biomass, and reduce P release from cells, resulting in lower P availability for plants [23]. Although sequential fractionation alone does not fully capture biogeochemical complexity of P cycling [88], integrating it with metagenomics and mass-spectrometry offers a more comprehensive understanding. Accordingly, our findings suggest that labile and moderately labile P fractions are important pools regulated by key P-cycling pathways, such as purine and pyrimidine metabolism, along with CHP and CHOSP compounds. These processes are strongly associated with copiotrophic taxa such as Actinobacteriota and Pseudomonadota [89], which contribute to organic matter turnover and restoration of soil health. Given that soil organic matter is a key determinant

of labile P availability [90, 91], we emphasize that both quantity and composition of organic matter determinates microbial access to resource for effective P cycling.

5. Conclusions

Long-term conversion of primary forest into agroforest or citrus plantation has significantly altered soil attributes and microbial functions associated to P cycling. Both microbial and LMWC compositions were strongly shaped by land use, which in turn influenced the potential for microbial P-cycling. Genes associated to "P acquisition" (e.g., transporters, phosphonate metabolism) were more abundant in agroforest soils compared to citrus plantation and had a positive correlation with moderate labile P fractions. In contrast, genes linked to "P-compounds synthesis" (e.g., pyrimidine metabolism, oxidative phosphorylation) were enriched in citrus plantation and negatively correlated with the labile P fraction. Despite the higher organic P fraction in citrus plantation soils, acid phosphatase activity was greater in the primary forest and the agroforest, suggesting that fertilization may suppress microbial P mineralization [92].

Agroforest with low management intensity consistently exhibited intermediate levels of P fractions, microbial and LMWC composition and enzymatic activity compared to primary forest and citrus plantation with high management intensity. This supports both plant productivity and nutrient cycling in these nutrient-poor soils. These patterns highlight the adaptability of microbial communities in accessing and using P, with functions prioritized based on resource availability. This was further evidenced in LMWC composition: primary forest and agroforest soils were enriched with nutrient-rich compounds, whereas citrus plantation soils contained more nutrient-poor compounds. By integrating genomic, metabolic, and environmental data, this study offers novel insights into the microbial mechanisms of P-cycling in tropical soils and highlights the role of LMWC in further supporting this process. Overall, managing microbial functions and

LMWC composition offers a promising path for improving P-use efficiency and promoting sustainable agriculture in the Amazon, where P is a finite and limited resource. However, our findings represent a temporal snapshot and may vary with seasonality, soil types, and different land management.

Acknowledgments

We would like to express our gratitude to Eduardo Vasconcelos for his maintenance of the agroforest and the citrus plantation site since the beginning of the experiment, to Lucas Franhani Alexandre for his help with the soil sampling campaign, and to Vitor Fernando Barro for his help with the soil enzyme analysis.

Funding

This study was financially suporte by the Fundação de Amparo à Pesquisa do Estado de São Paulo (FAPESP) and Fundação de Amparo à Pesquisa do Estado do Amazonas (FAPEAM) (projects 2020/08927-0; 2022/05561-0; 2024/06334-2; 2024/02443-1; 2021/10626-0). ML gratefully acknowledges funding by the Zwillenberg-Tietz Foundation.

Author Contributions

GLM: conceptualization, formal analysis, investigation, methodology, visualization, writing – original draft, writing – review & editing; **GGTNM**: formal analysis, validation, writing – review & editing; **ML**: validation, writing – review & editing; **ASF**: validation, writing – review & editing; **LNSB**: investigation, validation; **JvL**: data curation, writing – review & editing; **JECS**: data curation; **REH**: funding acquisition, writing – review & editing; **GG**: supervision, methodology, validation, writing – review & editing; **SMT**: conceptualization, funding acquisition, project administration, resources, supervision, validation, writing – review & editing.

Data availability statement

The datasets generated during and/or analyzed during the current study are available in the Zenodo repository: doi.org/10.5281/zenodo.15147497.

Conflict of interest

The authors declare that they have no known competing financial interests or personal relationships that could have appeared to influence the work reported in this paper.

References

1. Venturini AM et al. Soil microbes under threat in the Amazon Rainforest. *Trends in Ecology & Evolution* 2023;**38**:693–696.
2. Mueller RC et al. Links between plant and fungal communities across a deforestation chronosequence in the Amazon rainforest. *ISME Journal* 2014;**8**:1548–1550. https://doi.org/10.1038/ismej.2013.253
3. Rousseau G et al. Potential of slash-and-mulch system with legumes to conserve soil attributes and macrofauna diversity in Eastern Amazon. *Pedobiologia* 2022;**95**. https://doi.org/10.1016/j.pedobi.2022.150840
4. Celentano D et al. Carbon sequestration and nutrient cycling in agroforestry systems on degraded soils of Eastern Amazon, Brazil. *Agroforestry Systems* 2020;**94**:1781–1792. https://doi.org/10.1007/s10457-020-00496-4
5. Bieluczyk W et al. Slash-and-burn agriculture disrupts the carbon storage potential and ecosystem multifunctionality of Amazon's secondary forests. *Agriculture, Ecosystems and Environment* 2025;**381**. https://doi.org/10.1016/j.agee.2024.109413

6. Bonilla-Bedoya S et al. Effects of Land Use Change on Soil Quality Indicators in Forest Landscapes of the Western Amazon. *Soil Science* 2017;**182**:128–136. https://doi.org/10.1097/SS.0000000000000203

7. Lambers H. Phosphorus Acquisition and Utilization in Plants. *Annual Review of Plant Biology* 2022;**73**:17–42. https://doi.org/10.1146/annurev-arplant-102720-125738

8. Quesada CA et al. Basin-wide variations in Amazon forest structure and function are mediated by both soils and climate. *Biogeosciences* 2012;**9**:2203–2246. https://doi.org/10.5194/bg-9-2203-2012

9. Pedrinho A et al. Impacts of deforestation and forest regeneration on soil bacterial communities associated with phosphorus transformation processes in the Brazilian Amazon region. *Ecological Indicators* 2023;**146**. https://doi.org/10.1016/j.ecolind.2022.109779

10. Cunha HFV et al. Direct evidence for phosphorus limitation on Amazon forest productivity. *Nature* 2022;**608**:558–562. https://doi.org/10.1038/s41586-022-05085-2

11. Reichert T et al. Plant phosphorus-use and -acquisition strategies in Amazonia. *New Phytologist* 2022;**234**:1126–1143. https://doi.org/10.1111/nph.17985

12. Leite MFA et al. Microbiome resilience of Amazonian forests: Agroforest divergence to bacteria and secondary forest succession convergence to fungi. *Global Change Biology* 2023;**29**:1314–1327. https://doi.org/10.1111/gcb.16556

13. Soltangheisi A et al. Forest conversion to pasture affects soil phosphorus dynamics and nutritional status in Brazilian Amazon. *Soil and Tillage Research* 2019;**194**:104330. https://doi.org/10.1016/j.still.2019.104330

14. Roth VN et al. Persistence of dissolved organic matter explained by molecular changes during its passage through soil. *Nature Geoscience* 2019;**12**:755–761. https://doi.org/10.1038/s41561-019-0417-4

15. Schroeter SA et al. Microbial community functioning during plant litter decomposition. *Scientific Reports* 2022;**12**. https://doi.org/10.1038/s41598-022-11485-1

16. Gmach MR et al. Processes that influence dissolved organic matter in the soil: a review. *Scientia Agricola* 2019;**77**:2020. https://doi.org/10.1590/1678-992X-2018-0164

17. Liang C, Schimel JP, Jastrow JD. The importance of anabolism in microbial control over soil carbon storage. *Nature Microbiology* 2017;**2**:1–6. https://doi.org/10.1038/nmicrobiol.2017.105

18. Lange DF et al. Cycling of dissolved organic nutrients and indications for nutrient limitations in contrasting Amazon rainforest ecosystems. *Biogeochemistry* 2024;**167**:1567–1588. https://doi.org/10.1007/s10533-024-01187-3

19. Lange M et al. Plant diversity enhances production and downward transport of biodegradable dissolved organic matter. *Journal of Ecology* 2021;**109**:1284–1297. https://doi.org/10.1111/1365-2745.13556

20. Zeng J et al. PCycDB: a comprehensive and accurate database for fast analysis of phosphorus cycling genes. *Microbiome* 2022;**10**:1–16. https://doi.org/10.1186/s40168-022-01292-1

21. Liang JL et al. Novel phosphate-solubilizing bacteria enhance soil phosphorus cycling following ecological restoration of land degraded by mining. *ISME Journal* 2020;**14**:1600–1613. https://doi.org/10.1038/s41396-020-0632-4

22. Dai Z et al. Long-term nutrient inputs shift soil microbial functional profiles of phosphorus cycling in diverse agroecosystems. *ISME Journal* 2020;**14**:757–770. https://doi.org/10.1038/s41396-019-0567-9

23. Chen J et al. Microbial phosphorus recycling in soil by intra- and extracellular mechanisms. *ISME Communications* 2023;**3**:135. https://doi.org/10.1038/s43705-023-00340-7

24. Alvares CA et al. Köppen's climate classification map for Brazil. *Meteorologische Zeitschrift* 2013;**22**:711–728. https://doi.org/10.1127/0941-2948/2013/0507

25. WRB-IUSS. World Reference Base for Soil Resources. World Soil Resources Reports 106. *World Soil Resources Reports No. 106* . 2014.

26. Pitman NCA et al. DOMINANCE AND DISTRIBUTION OF TREE SPECIES IN UPPER AMAZONIAN TERRA FIRME FORESTS. *Ecology* 2001;**82**:2101–2117. https://doi.org/10.1890/0012-9658(2001)082%255B2101:DADOTS%255D2.0.CO;2

27. Sokol NW et al. Life and death in the soil microbiome: how ecological processes influence biogeochemistry. *Nature Reviews Microbiology* 2022;**0123456789**. https://doi.org/10.1038/s41579-022-00695-z

28. Raij B van et al. Análise química para avaliação da fertilidade de solos tropicais. *Campinas: Instituto Agronômico* . 2001.

29. Teixeira PC et al. Manual de Métodos de Análise de Solo. Brasília, DF: EMBRAPA, 2017.

30. Eivazi F, Tabatabai MA. Glucosidases and galactosidases in soils. *Soil Biology and Biochemistry* 1988;**20**:601–606. https://doi.org/10.1016/0038-0717(88)90141-1

31. Tabatabai MA, Bremner JM. Use of p-nitrophenyl phosphate for assay of soil phosphatase activity. *Soil Biology and Biochemistry* 1969;**1**:301–307. https://doi.org/10.1016/0038-0717(69)90012-1

32. Tabatabai MA, Bremner JM. Arylsulfatase Activity of Soils. *Soil Science Society of America Journal* 1970;**34**:225–229. https://doi.org/10.2136/sssaj1970.03615995003400020016x

33. Hedley MJ, Stewart JWB, Chauhan BS. Changes in Inorganic and Organic Soil Phosphorus Fractions Induced by Cultivation Practices and by Laboratory Incubations. *Soil Science Society of America Journal* 1982;**46**:970–976. https://doi.org/10.2136/sssaj1982.03615995004600050017x

34. Gatiboni LC, Condron LM. A rapid fractionation method for assessing key soil phosphorus parameters in agroecosystems. *Geoderma* 2021;**385**:114893. https://doi.org/10.1016/j.geoderma.2020.114893

35. Murphy J, Riley JP. A modified single solution method for the determination of phosphate in natural waters. *Analytica Chimica Acta* 1962;**27**:31–36. https://doi.org/10.1016/S0003-2670(00)88444-5

36. Jones DL, Willett VB. Experimental evaluation of methods to quantify dissolved organic nitrogen (DON) and dissolved organic carbon (DOC) in soil. *Soil Biology and Biochemistry* 2006;**38**:991–999. https://doi.org/10.1016/j.soilbio.2005.08.012

37. Dittmar T et al. A simple and efficient method for the solid-phase extraction of dissolved organic matter (SPE-DOM) from seawater. *Limnology and Oceanography: Methods* 2008;**6**:230–235. https://doi.org/10.4319/lom.2008.6.230

38. Simon C et al. Molecular Signals of Heterogeneous Terrestrial Environments Identified in Dissolved Organic Matter: A Comparative Analysis of Orbitrap and Ion

Cyclotron Resonance Mass Spectrometers. *Frontiers in Earth Science* 2018;**6**. https://doi.org/10.3389/feart.2018.00138

39. Schroeter SA et al. Hydroclimatic extremes threaten groundwater quality and stability. *Nature communications* 2025;**16**:720. https://doi.org/10.1038/s41467-025-55890-2
40. Hulstaert N et al. ThermoRawFileParser: Modular, Scalable, and Cross-Platform RAW File Conversion. *Journal of Proteome Research* 2020;**19**:537–542. https://doi.org/10.1021/acs.jproteome.9b00328
41. Schum SK, Brown LE, Mazzoleni LR. MFAssignR: Molecular formula assignment software for ultrahigh resolution mass spectrometry analysis of environmental complex mixtures. *Environmental Research* 2020;**191**:110114. https://doi.org/10.1016/j.envres.2020.110114
42. Merder J et al. ICBM-OCEAN: Processing Ultrahigh-Resolution Mass Spectrometry Data of Complex Molecular Mixtures. *Anal Chem* 2020;**92**:6832–6838. https://doi.org/10.1021/acs.analchem.9b05659
43. Khatami S et al. Formation of water-soluble organic matter through fungal degradation of lignin. *Organic Geochemistry* 2019;**135**:64–70. https://doi.org/10.1016/j.orggeochem.2019.06.004
44. Koch BP, Dittmar T. Erratum: From mass to structure: An aromaticity index for high-resolution mass data of natural organic matter (Rapid Communications in Mass Spectrometry (2006) 20 (926-932) DOI: 10.1002/rcm.2386). *Rapid Communications in Mass Spectrometry* 2016;**30**:250. https://doi.org/10.1002/rcm.7433
45. Caporaso JG et al. Global patterns of 16S rRNA diversity at a depth of millions of sequences per sample. *Proceedings of the National Academy of Sciences of the*

United States of America 2011;**108**:4516–4522. https://doi.org/10.1073/pnas.1000080107

46. White TJ et al. Amplification and Direct Sequencing of Fungal Ribosomal Rna Genes for Phylogenetics. *PCR Protocols* 1990;315–322. https://doi.org/10.1016/b978-0-12-372180-8.50042-1
47. Ewels PA et al. The nf-core framework for community-curated bioinformatics pipelines. *Nature Biotechnology* 2020;**38**:276–278. https://doi.org/10.1038/s41587-020-0439-x
48. Straub D et al. Interpretations of Environmental Microbial Community Studies Are Biased by the Selected 16S rRNA (Gene) Amplicon Sequencing Pipeline. *Frontiers in Microbiology* 2020;**11**:1–18. https://doi.org/10.3389/fmicb.2020.550420
49. Callahan BJ et al. DADA2: High-resolution sample inference from Illumina amplicon data. *Nature Methods* 2016;**13**:581–583. https://doi.org/10.1038/nmeth.3869
50. Nilsson RH et al. The UNITE database for molecular identification of fungi: Handling dark taxa and parallel taxonomic classifications. *Nucleic Acids Research* 2019;**47**:D259–D264. https://doi.org/10.1093/nar/gky1022
51. Xue CX et al. DiTing: A Pipeline to Infer and Compare Biogeochemical Pathways From Metagenomic and Metatranscriptomic Data. *Frontiers in Microbiology* 2021;**12**:1–15. https://doi.org/10.3389/fmicb.2021.698286
52. Li D et al. MEGAHIT: An ultra-fast single-node solution for large and complex metagenomics assembly via succinct de Bruijn graph. *Bioinformatics* 2015;**31**:1674–1676. https://doi.org/10.1093/bioinformatics/btv033
53. Hyatt D et al. Integrated nr Database in Protein Annotation System and Its Localization. *Nature Communications* 2010;**6**:1–8.

54. Alboukadel Kassambara. Package 'factoextra' - Extract and Visualize the Results of Multivariate Data Analyses. 2022.

55. Oksanen J et al. Package 'vegan' Title Community Ecology Package. 2019.

56. Gloor G. ALDEx2: ANOVA-Like Differential Expression tool for compositional data. *Bioconductor* 2018;**1**:1–10.

57. Tenenhaus M et al. PLS path modeling. *Computational Statistics and Data Analysis* 2005;**48**:159–205. https://doi.org/10.1016/j.csda.2004.03.005

58. Sanchez G. PLS Path Modeling with R. *R Package Notes* . 2013.

59. Siles JA et al. Long-term restoration with organic amendments is clearer evidenced by soil organic matter composition than by changes in microbial taxonomy and functionality. *Applied Soil Ecology* 2024;**198**:105383. https://doi.org/10.1016/j.apsoil.2024.105383

60. Wu X et al. Genome-Resolved Metagenomics Reveals Distinct Phosphorus Acquisition Strategies between Soil Microbiomes. *mSystems* 2022;**7**:e01107-21. https://doi.org/10.1128/msystems.01107-21

61. Goss-Souza D et al. Amazon forest-to-agriculture conversion alters rhizosphere microbiome composition while functions are kept. *FEMS Microbiology Ecology* 2019;**95**:1–13. https://doi.org/10.1093/femsec/fiz009

62. Merloti LF et al. Long-term land use in Amazon influence the dynamic of microbial communities in soil and rhizosphere. *Rhizosphere* 2022;**21**. https://doi.org/10.1016/j.rhisph.2022.100482

63. Guigue J et al. Water-extractable organic matter linked to soil physico-chemistry and microbiology at the regional scale. *Soil Biology and Biochemistry* 2015;**84**:158–167. https://doi.org/10.1016/j.soilbio.2015.02.016

64. Gómez AIP et al. Unveiling soil bacterial diversity in the Andes-Amazon transition zone: Impacts of forest conversion to pasture. *Applied Soil Ecology* 2024;**201**. https://doi.org/10.1016/j.apsoil.2024.105486

65. Lammel DR et al. Direct and indirect effects of a pH gradient bring insights into the mechanisms driving prokaryotic community structures. *Microbiome* 2018;**6**:7–9. https://doi.org/10.1186/s40168-018-0482-8

66. Kidinda LK et al. Relationships between geochemical properties and microbial nutrient acquisition in tropical forest and cropland soils. *Applied Soil Ecology* 2023;**181**:104653. https://doi.org/10.1016/j.apsoil.2022.104653

67. Oelmann Y et al. Above- and belowground biodiversity jointly tighten the P cycle in agricultural grasslands. *Nature Communications* 2021;**12**:1–9. https://doi.org/10.1038/s41467-021-24714-4

68. Peng Z et al. Land conversion to agriculture induces taxonomic homogenization of soil microbial communities globally. *Nature Communications* 2024;**15**:1–13. https://doi.org/10.1038/s41467-024-47348-8

69. Liu H et al. Effects of the interaction between temperature and revegetation on the microbial degradation of soil dissolved organic matter (DOM) – A DOM incubation experiment. *Geoderma* 2019;**337**:812–824. https://doi.org/10.1016/j.geoderma.2018.10.041

70. Yang Y et al. Deciphering factors driving soil microbial life-history strategies in restored grasslands. *iMeta* 2023;**2**:1–21. https://doi.org/10.1002/imt2.66

71. Navarrete AA et al. Acidobacterial community responses to agricultural management of soybean in Amazon forest soils. *FEMS Microbiology Ecology* 2013;**83**:607–621. https://doi.org/10.1111/1574-6941.12018

72. Pedrinho A et al. Forest-to-pasture conversion and recovery based on assessment of microbial communities in Eastern Amazon rainforest. *FEMS Microbiology Ecology* 2019;**95**:1–10. https://doi.org/10.1093/femsec/fiy236

73. Manici LM et al. Ascomycota and Basidiomycota fungal phyla as indicators of land use efficiency for soil organic carbon accrual with woody plantations. *Ecological Indicators* 2024;**160**:111796. https://doi.org/10.1016/j.ecolind.2024.111796

74. Stone BWG et al. Life history strategies among soil bacteria—dichotomy for few, continuum for many. *ISME Journal* 2023;**17**:611–619. https://doi.org/10.1038/s41396-022-01354-0

75. Duan P et al. Tree species diversity increases soil microbial carbon use efficiency in a subtropical forest. *Global Change Biology* 2023;**29**:7131–7144. https://doi.org/10.1111/gcb.16971

76. Tong H et al. Land-Use Change and Environmental Properties Alter the Quantity and Molecular Composition of Soil-Derived Dissolved Organic Matter. *ACS Earth and Space Chemistry* 2021;**5**:1395–1406. https://doi.org/10.1021/acsearthspacechem.1c00033

77. Man M, Simpson MJ. Dissolved organic matter molecular composition controls potential biodegradability. *Organic Geochemistry* 2025;**200**:104924. https://doi.org/10.1016/j.orggeochem.2024.104924

78. Freeman EC et al. Universal microbial reworking of dissolved organic matter along environmental gradients. *Nature Communications* 2024;**15**. https://doi.org/10.1038/s41467-023-44431-4

79. Ye Q et al. Dissolved organic matter characteristics in soils of tropical legume and non-legume tree plantations. *Soil Biology and Biochemistry* 2020;**148**:107880. https://doi.org/10.1016/j.soilbio.2020.107880

80. Sangmanee P et al. Organic carbon compounds associated with deep soil carbon stores. *Plant Soil* 2023;**488**:83–99. https://doi.org/10.1007/s11104-022-05627-7

81. Quesada CA et al. Soils of Amazonia with particular reference to the RAINFOR sites. *Biogeosciences* 2011;**8**:1415–1440. https://doi.org/10.5194/bg-8-1415-2011

82. Gomes MF et al. Soil health indicators in oil palm agroforestry systems in the eastern Amazon, Brazil. *Geoderma Regional* 2024;**37**. https://doi.org/10.1016/j.geodrs.2024.e00806

83. Visscher AM et al. Biological soil health indicators are sensitive to shade tree management in a young cacao (Theobroma cacao L.) production system. *Geoderma Regional* 2024;**37**:e00772. https://doi.org/10.1016/j.geodrs.2024.e00772

84. Schaap KJ et al. Litter inputs and phosphatase activity affect the temporal variability of organic phosphorus in a tropical forest soil in the Central Amazon. *Plant and Soil* 2021;**469**:423–441. https://doi.org/10.1007/s11104-021-05146-x

85. Margenot AJ, Sommer R, Parikh SJ. Soil Phosphatase Activities across a Liming Gradient under Long-Term Managements in Kenya. *Soil Science Soc of Amer J* 2018;**82**:850–861. https://doi.org/10.2136/sssaj2017.12.0420

86. Gan HY et al. Soil Organic Matter Mineralization as Driven by Nutrient Stoichiometry in Soils Under Differently Managed Forest Stands. *Front For Glob Change* 2020;**3**:99. https://doi.org/10.3389/ffgc.2020.00099

87. Gu C, Margenot AJ. Navigating limitations and opportunities of soil phosphorus fractionation. *Plant and Soil* 2021;**459**:13–17. https://doi.org/10.1007/s11104-020-04552-x

88. Gama-Rodrigues AC et al. An exploratory analysis of phosphorus transformations in tropical soils using structural equation modeling. *Biogeochemistry* 2014;**118**:453–469. https://doi.org/10.1007/s10533-013-9946-x

89. Lipa P, Janczarek M. Phosphorylation systems in symbiotic nitrogen-fixing bacteria and their role in bacterial adaptation to various environmental stresses. *PeerJ* 2020;**8**. https://doi.org/10.7717/peerj.8466

90. Johnson AH, Frizano J, Vann DR. Biogeochemical implications of labile phosphorus in forest soils determined by the Hedley fractionation procedure. *Oecologia* 2003;**135**:487–499. https://doi.org/10.1007/s00442-002-1164-5

91. Boitt G et al. Impacts of long-term plant biomass management on soil phosphorus under temperate grassland. *Plant and Soil* 2018;**427**:163–174. https://doi.org/10.1007/s11104-017-3429-0

92. Yu Q et al. Long-term phosphorus addition inhibits phosphorus transformations involved in soil arbuscular mycorrhizal fungi and acid phosphatase in two tropical rainforests. *Geoderma* 2022;**425**:116076. https://doi.org/10.1016/j.geoderma.2022.116076

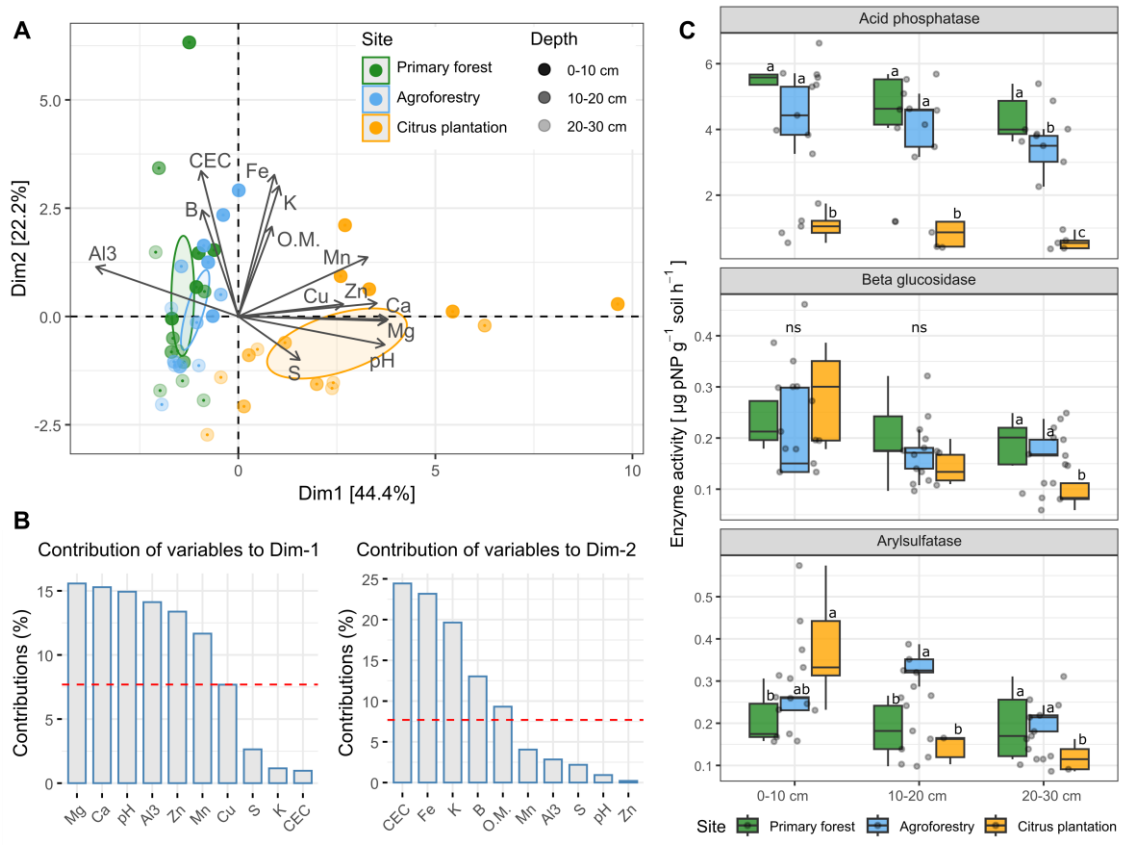

Fig. 1. (A) Principal component analysis (PCA) of soil chemical attributes across land-use systems. Ellipses represent the 95% confidence interval. (B) Variables contribution to the first and second dimension of the PCA. Dashed red line indicates the significant threshold of variables. (C) Soil enzymatic activity across land-use systems at different soil depths. Boxplots show mean, median, and 95% confidence interval (n = 5). Letters indicate significant differences between land-use systems at the same soil depth by the Kruskal-Wallis test followed by Dunn's post-hoc ($p < 0.05$). Asterisks indicate significant differences between soil depths by one-way ANOVA (** = $p < 0.01$; * = $p < 0.05$).

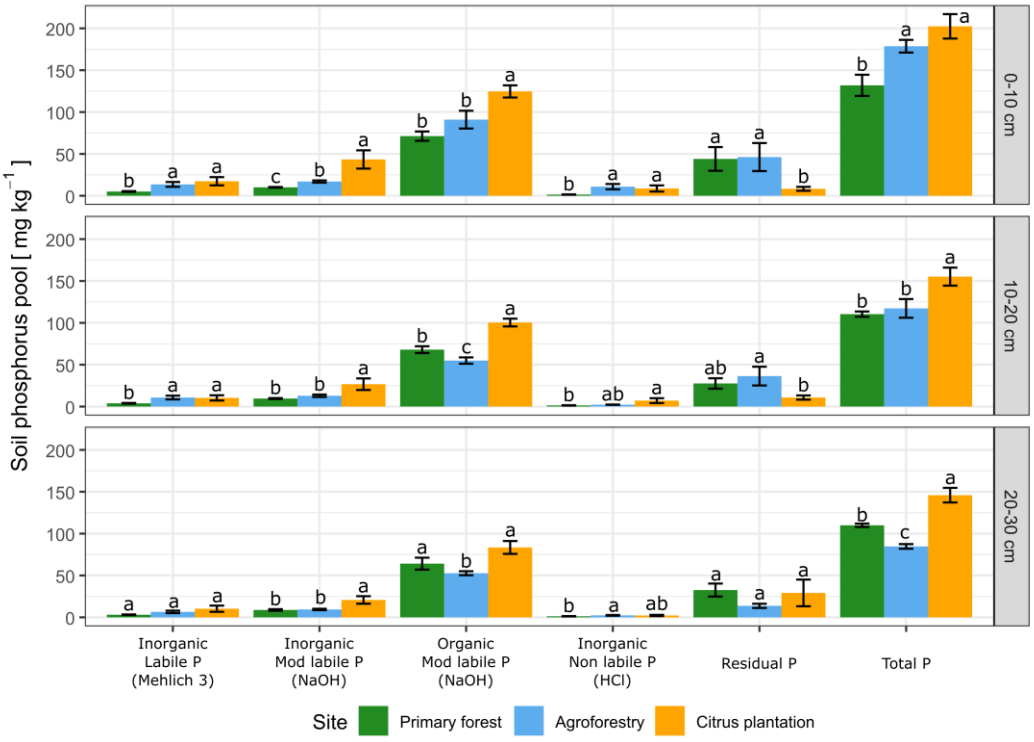

Fig. 2. Soil phosphorus fractions in different soil depths across land-use systems. Fractions are shown in their sequential extraction order. Data are mean ± SE (n = 5). Letters indicate significant differences between land-use systems by the Kruskal-Wallis test followed by Dunn's post-hoc ($p < 0.05$).

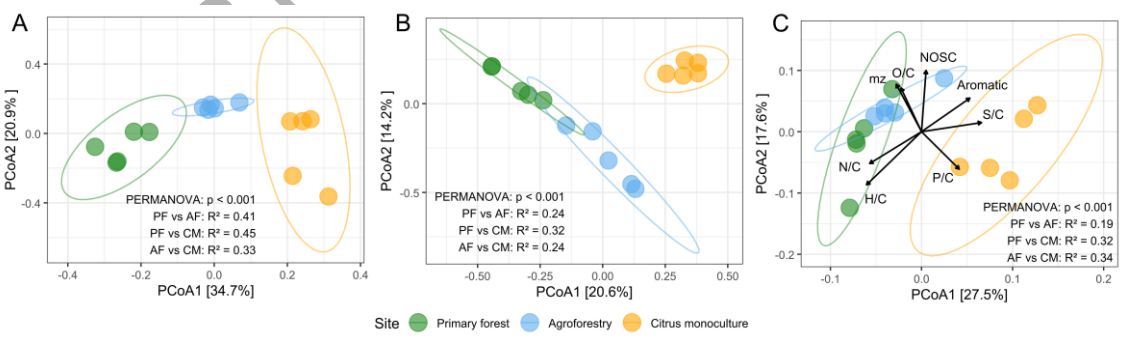

Fig. 3. (A) Bacterial, (B) fungal community, and (C) Low molecular weight organic compounds (LMWC) composition across land-use systems represented by a Principal

Coordinate Analysis (PCoA) based on Bray-Curtis dissimilarity. Arrows indicate intensity-weighted LMWC parameters, fitted as vectors. Coefficients of determination (R^2) denote the proportion of variance explained by the model.

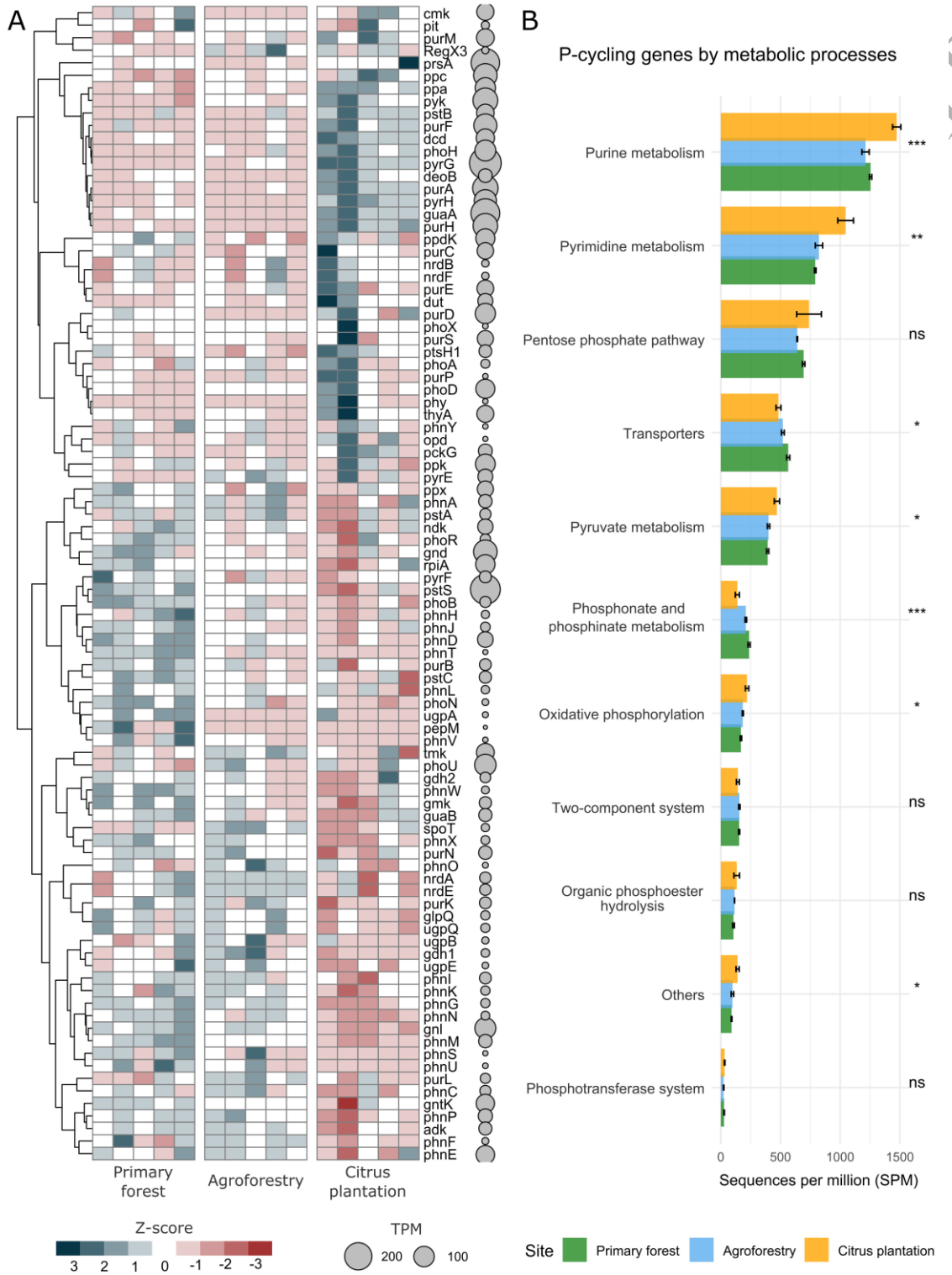

Fig. 4. (A) Heatmap showing the abundance of phosphorus cycling genes in different land-use change systems. Colors from blue to red represents a range from high to low abundance of sequences per million (SPM) normalized by z-score. (B) Barplot showing the metabolic pathways involved in microbial phosphorus cycle represented by SPM. Data are mean ± SE (n = 5). Asterisk indicate significant differences among land-use systems by one-way ANOVA (*** = $p < 0.001$; ** = $p < 0.01$; * = $p < 0.05$).

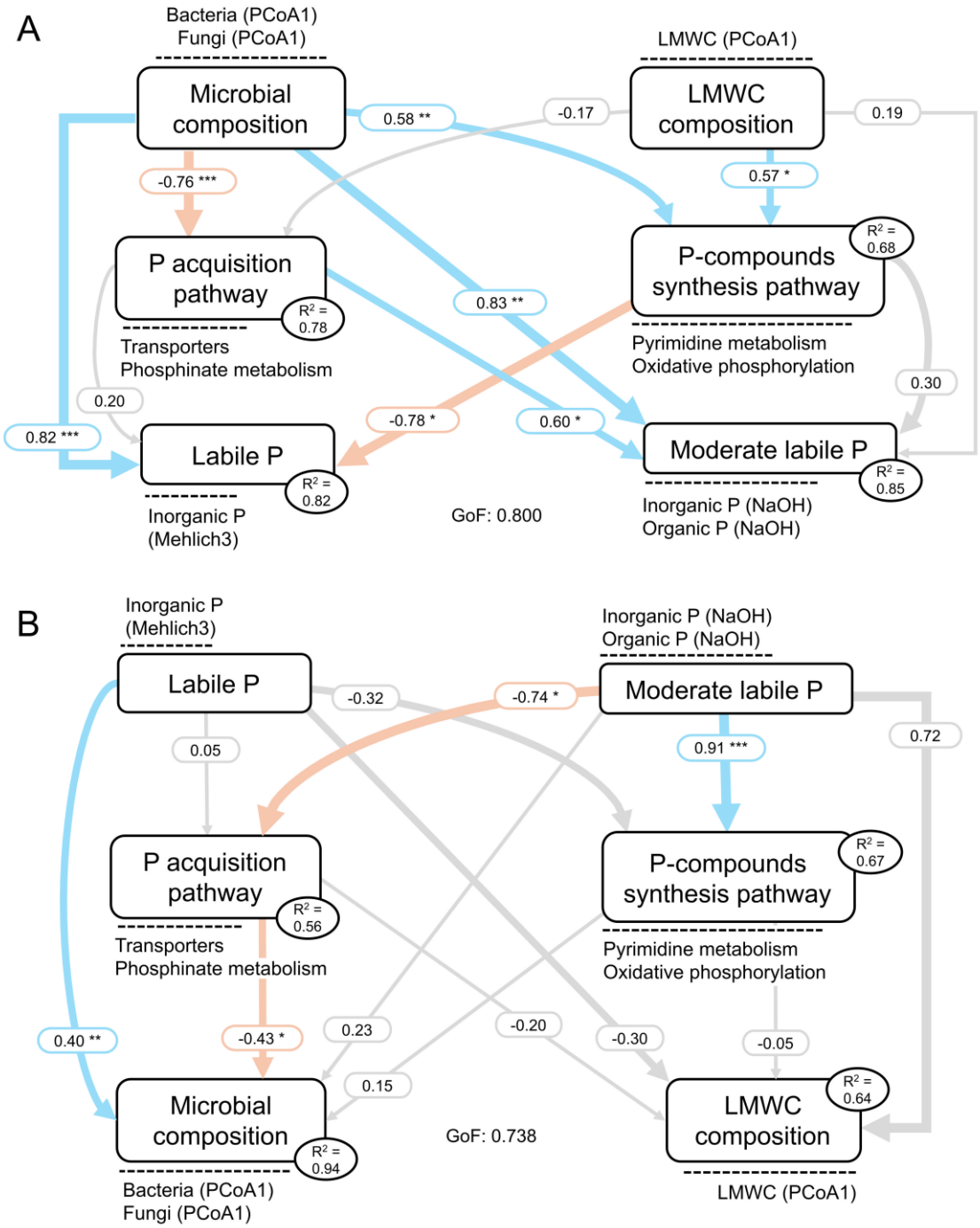

Fig. 5. (A) Partial least squares path modeling (PLS-PM) showing the direct effects of microbial and low molecular weight organic compounds (LMWC) composition on P-cycling pathways and P fractions. (B) PLS-PM showing the direct effects of P fractions on P-cycling pathways and microbial and LMWC composition. Boxes represent latent variables used in the PLS-PM and variables near the dashed lines represents the observed

variables. R^2 values are the coefficients of determination of the endogenous latent variables. Blue and orange arrows indicate significant positive and negative effects, respectively. Grey arrows indicate non-significant effects. Arrow width indicates the relationship strength. Numbers near the arrows indicate significant standardized path coefficient. Asterisks indicate significant effects (* = $p < 0.05$; ** = $p < 0.01$; *** = $p < 0.001$).

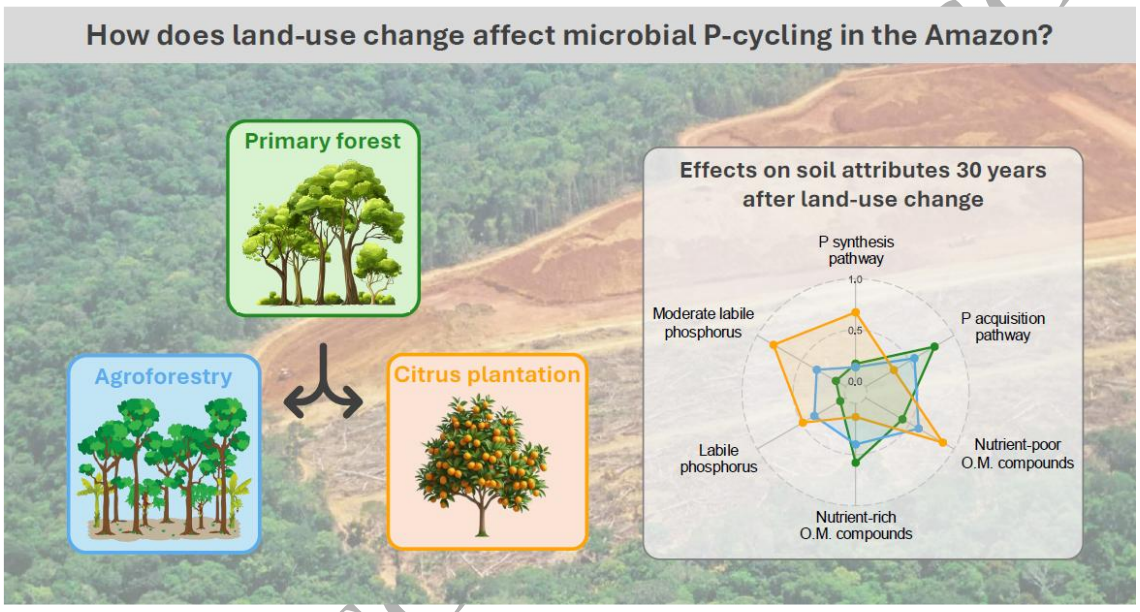

Graphical_abstract